

Full paper / Mémoire

Design of microporous materials: A novel generation of solid acids

Jaouad Arichi*, Svetlana Ivanova, Benoît Louis

Laboratoire des matériaux, surfaces et procédés pour la catalyse (LMSPC), UMR 7515 du CNRS, Université Louis-Pasteur, 25, rue Becquerel, 67087 Strasbourg cedex 2, France

Received 6 May 2008; accepted after revision 25 November 2008
Available online 12 February 2009

Abstract

ZSM-5 zeolite materials were synthesized under acidic conditions using a fluoride-mediated route. Our approach consisted in changing the nature of the silica source in the starting synthesis gel via two different pathways: (i) polymeric silica having different surface specific areas (aerosils 130, 200 and 300); and (ii) dissolution–recrystallization of a thin silica upper layer of a silicon carbide substrate. The zeolites were characterized by XRD, SEM, and H/D exchange titration methods. ^{27}Al MAS NMR analysis revealed that all aluminum was present in a tetrahedral coordination, thus being present inside the zeolite framework.

A complete self-transformation of aerosils 130, 200 and 300 sources into highly crystalline ZSM-5 material was achieved, thus leading to a star-like morphology for the MFI crystals. Hence, this study reports the first observation of this unusual star-like morphology for zeolite crystals. It is therefore possible to synthesize zeolites having properties tailored at the microscopic level. Finally, these structured materials were both active and selective catalysts in the conversion of methanol-to-gasoline (MTG process). **To cite this article: J. Arichi et al., C. R. Chimie 12 (2009).**

© 2008 Académie des sciences. Published by Elsevier Masson SAS. All rights reserved.

Résumé

Dans le présent travail nous proposons une nouvelle voie de préparation de cristaux de zéolithe ZSM-5 auto-assemblés. La synthèse de zéolithes a été effectuée en milieu fluoré et en choisissant judicieusement la composition du gel précurseur. La caractérisation du matériau par DRX, BET, SEM et RMN (^{27}Al) confirme la formation de la structure MFI.

La conversion du méthanol en hydrocarbures représente une source d'énergie alternative au pétrole. Ainsi nous avons utilisé la zéolithe ZSM-5 préparée pour cette réaction. Ce choix est dicté par le fait que les oléfines $\text{C}_2\text{--}\text{C}_4$ représentent des intermédiaires chimiques importants dans l'industrie, et par le fait que la sélectivité est contrôlée par le temps de contact des réactifs avec le catalyseur acide. **Pour citer cet article : J. Arichi et al., C. R. Chimie 12 (2009).**

© 2008 Académie des sciences. Published by Elsevier Masson SAS. All rights reserved.

Keywords: solid acids; ZSM-5 zeolite; self-structured materials; MTG process

Mots-clés : solide acide ; ZSM-5 zéolite ; MTG process

* Corresponding author.

E-mail address: arichij@ecpm.u-strasbg.fr (J. Arichi).

1. Introduction

A large number of catalytic materials are generally produced as powders with loosely bonded particles. Inorganic binders (silica, alumina) are often used for shaping the final material, in order to optimise both its mechanical strength and attrition resistance, and thus increase its lifetime. However, the use of those binders presents several drawbacks: the binder partly blocks the access to the catalyst active phase, which decreases the catalyst efficiency and raises diffusion limitations. During the past two decades, a huge interest in catalytic reactor engineering based on structured catalytic beds was grown [1]. Compared to traditional randomly packed-bed reactors, structured catalytic beds provide improved hydrodynamics. This leads to a narrower residence time distribution, improved control of consecutive reactions which results in higher product selectivity. Therefore, the development of novel materials suitable for the design of structured catalytic beds is highly desirable [1].

Zeolites materials are widely used in industrial heterogeneous catalysis. Among many zeolite structures as acid catalysts, zeolite ZSM-5 having the MFI type topology remains the material of choice for several acid catalyzed processes like fluid catalytic cracking (FCC) [2–11]. The presence of the aluminum atoms in the zeolite framework introduces negative charges, which are counter-balanced by protons. Hence, formed zeolite exhibits a strong Brønsted acidity. Structured ZSM-5 zeolite catalysts were prepared via a binderless hydrothermal synthesis on metals [2–5] or ceramics [6–11]. In spite of a reduced pressure drop, and improved heat and mass transfers when compared to extrudated pellets or powdered microgranules, the industrial applications of these structured materials are rather limited. This is either due to the lack of support inertness or to non-sufficient mechanical and chemical stabilities.

The aim of the present work is to report the synthesis of self-assembled ZSM-5 crystals, as valuable catalysts for petrochemical applications, by varying the nature of the silica source in the synthesis gel. Firstly, ZSM-5 crystals were directly grown on a silicon carbide support surface. Silicon carbide (SiC) indeed exhibits beneficial intrinsic properties: high thermal conductivity and mechanical strength, high resistance toward oxidation, chemical inertness, and ease of shaping [12,13]. Before the zeolite coating procedure, the SiC substrate material has to be activated by a thermal heat treatment at high temperature under air. A nanoscopic layer of SiO_x was formed on

its surface [27], which decreases the inertness and favours the deposition of the zeolite layer.

The second approach was to synthesize ZSM-5 crystals, from a barely soluble polymeric silica source to produce self-assembled crystals into defined morphologies.

Methanol-to-gasoline (MTG) was chosen as a test reaction, to investigate the impact of the silica source on the morphological properties of these micro-structured zeolite catalysts. Indeed, the size and shape of the MFI zeolite crystals govern the selectivity toward light olefins or saturated hydrocarbons [14].

2. Experimental

2.1. Strategy for ZSM-5 zeolite synthesis

2.1.1. Polymeric silica source

ZSM-5 samples were prepared from synthesis gels of molar composition TPA-Br:SiO₂:NaAlO₂:NH₄F:H₂O = 0.07:1:0.012:1.1:80 using sodium aluminate (52.5 wt% NaAlO₂, Riedel-de-Haën), tetrapropylammonium bromide as the structure-directing agent (TPA-Br, 99%, Merck-Suchardt), ammonium fluoride (NH₄F, >98%, Fluka) and deionised water as the solvent. Later on, the silica source aerosils 130, 200, 300 (Degussa Evonik), were introduced under vigorous stirring. A few drops of hydrofluoric solution (40 wt%) were added to decrease the alkalinity of the solution to pH = 5. The mixture was homogenised and aged during 2 h. The gel was then poured into a Teflon-lined autoclave and maintained at 443 K for 147 h. The crystalline material was filtered, washed with demineralised water and dried at 393 K. The H-forms were obtained after calcinations in air for 5 h at 773 K.

2.1.2. Silicon oxy-carbide transformation

Silicon carbide was prepared by gas–solid reaction between solid carbon and SiO vapours in the temperature range 1200–1400 °C according to the shape memory synthesis developed by Ledoux et al. [12,13,15]. This method allows the synthesis of silicon carbide with different sizes and shapes, depending on their subsequent uses. Prior to the synthesis, the support was calcined at 1173 K for 2 h in order to form a nanoscopic layer of SiO₂ on its surface (10 wt%). This layer will provide the reservoir of SiO₂ nutrient for the zeolite synthesis.

The zeolite synthesis mixture was prepared by dissolving the TPA-Br template in deionised water and stirring for 10 min. The gel was stirred during further addition of ammonium fluoride for 15 min. Then,

sodium aluminate was added to the gel for 15 min. The reactants were mixed according to the following composition: $\text{NaAlO}_2\text{:TPA-Br:NH}_4\text{F:H}_2\text{O} = 1\text{:6:184:6538}$, respectively. Then the $\beta\text{-SiC}$ powder support was placed in the solution, and the solution was aged for 3 h. The synthesis was performed at 443 K under autogeneous pressure for 147 h. After hydrothermal synthesis, the solid material was dried at 373 K. Afterwards, both the organic template and ammonia were removed by treating the material in air at 773 K for 5 h.

2.2. Characterization techniques

X-ray diffraction patterns (XRD) were recorded on a Bruker D8 Advance diffractometer, with a Ni detector side filtered $\text{Cu K}\alpha$ radiation (1.5406 Å) over a 2θ range of $5\text{--}50^\circ$ and a position sensitive detector using a step size of 0.02° and a step time of 2 s. XRD was used to validate the synthesis procedure, with respect to the crystalline structure while comparing the patterns obtained with the JCPDS tables.

Specific surface areas (SSA) of the different zeolites were determined by N_2 adsorption–desorption measurements at 77 K using BET-method (Micromeritics sorptometer Tri Star 3000). Prior to nitrogen adsorption, the samples were outgassed at 573 K for 4 h in order to desorb moisture adsorbed on the surface and inside the porous network.

Scanning electron microscopy (SEM) micrographs were recorded on a JEOL FEG 6700F microscope working at 9 kV accelerating voltage. Before observation, the sample was covered by a carbon layer to decrease the charge effect during the analysis.

^{27}Al ($I = 5/2$) magic angle spinning nuclear magnetic resonance (MAS NMR) was carried out on a Bruker DSX 400 spectrometer operating at $B_0 = 9.4$ T (Larmor frequency $\nu_0 = 104.2$ MHz). A single pulse of $0.7\ \mu\text{s}$ with a recycle delay of 300 ms was used for all experiments. The spinning frequency was 10 kHz. Measurements were carried out at room temperature with $[\text{Al}(\text{H}_2\text{O})_6]^{3+}$ as external standard reference.

The Brönsted acidity of the materials was evaluated using our H/D isotope-exchange technique reported elsewhere [16]. This technique also allows the precise determination of the number of O–H groups in as-synthesized zeolites after calcination of the template, ion-exchange process, and again calcination [16].

2.3. Catalytic tests

The methanol-to-gasoline (MTG) reaction was performed at atmospheric pressure and 673 K using a fixed-

bed quartz reactor packed with 4 g of catalyst and a mixture of $0.5\ \text{ml min}^{-1}$ methanol and $60\ \text{ml min}^{-1}$ in argon. The methanol was fed by means of a HPLC pump, followed by vaporisation at 423 K in argon flow. The analyses were performed by gas chromatography to quantify the concentration of hydrocarbons with a FID detector and DB-1 column (30 m long and 0.53 mm internal diameter). The temperature was controlled by means of two thermocouples placed inside and outside the reactor system.

3. Results and discussion

3.1. Structural characterizations

The zeolites produced via the fluoride route are usually pure crystalline phases [17,18], with a narrow crystal size distribution, when compared to the hydroxide-mediated route [19]. Fig. 1 presents the XRD of H-[F]ZSM-5 zeolite grown upon dispersed polymeric silica gel (aerosils 130, 200 and 300). The material exhibits the characteristic pattern of the MFI structure [20]. Moreover, no distortion of the base line of the XRD pattern was observed, which indicates that the quantity of any present amorphous silica (non-transformed silica source: aerosils 130, 200 and 300) is below detection limit of 5% for the sXRD apparatus. Furthermore, the yield of zeolite synthesis (based on Si) was about 80% with aerosil (130, 200 and 300) as silica sources. This value is higher than the 60–70% yield achieved with TEOS source. Thereby, one can expect that a complete self-transformation was therefore reached for the polymeric aerosil silica sources into ZSM-5 zeolite. Similar XRD pattern was obtained for the crystals grown on the $\beta\text{-SiC}$ surface, indicating the formation of ZSM-5 zeolite. Nevertheless, the

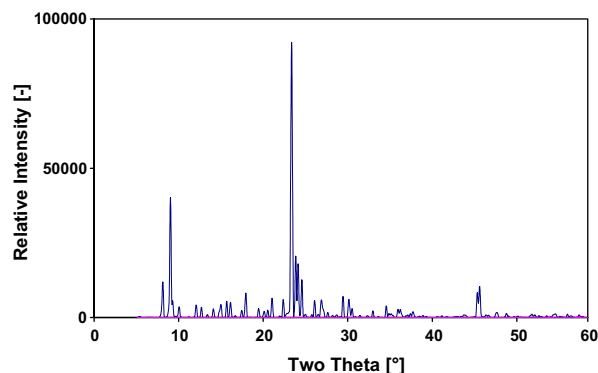


Fig. 1. XRD pattern of H-[F]ZSM-5 grown upon the polymeric aerosil silica source.

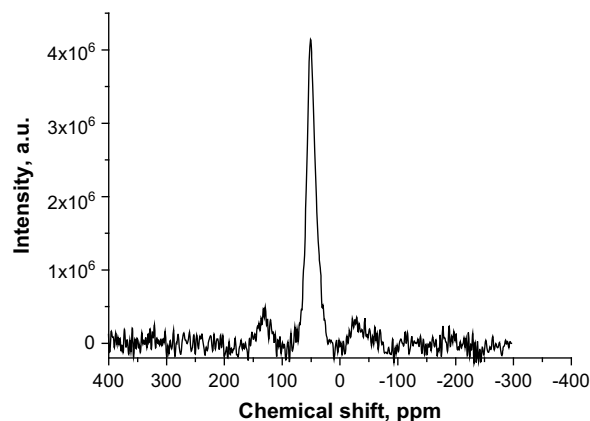


Fig. 2. ^{27}Al MAS NMR spectra of the obtained zeolite showing the presence of AlO_4 tetrahedra which are typical features of zeolites.

presence of the β -SiC material weakens the intensities of the obtained diffraction peaks.

The ^{27}Al MAS NMR spectra of the composite material ZSM-5/ β -SiC prepared during 147 h is shown in Fig. 2. A single and narrow signal was observed at 52 ppm, which can unambiguously be attributed to tetrahedrally coordinated aluminum atoms in the zeolite framework [21–22]. Furthermore, the absence of any signal at 0 ppm indicates the absence of any extra-framework aluminum species. Indeed, all aluminum atoms were successfully incorporated into the MFI zeolite framework. The ^{27}Al NMR spectra, combined with the obtained XRD MFI patterns, confirm the presence of a zeolite framework containing AlO_4 tetrahedra.

The zeolite acid properties are directly related to its aluminum content. Therefore, the Brønsted acidity of the different zeolite was investigated by means of H/D isotope-exchange technique [16,23]. The bare β -SiC substrate exhibits only a limited amount of OH groups, $0.110 \text{ mmol g}^{-1}$ SiC. After synthesis duration of 147 h, the total number of Brønsted acid sites was increased to $0.414 \text{ mmol g}^{-1}$ composite. Hence, based on H/D exchange experiments, the amount of zeolite crystals present on the β -SiC surface support was found to be 15 wt%.

Furthermore, the determined SSA for the ZSM-5 zeolite obtained by complete transformation of the polymeric silica (aerosils 130, 200 and 300) is $350 \text{ m}^2/\text{g}$, which is the usual reported value for highly crystalline ZSM-5. Bare β -SiC have no porosity, meanwhile, the obtained SSA value for ZSM-5/ β -SiC composite is $55 \text{ m}^2/\text{g}$. This increase in the SSA values can be connected with the generation of micropores, which are absent in the bare β -SiC silica source, but are typical for zeolite materials.

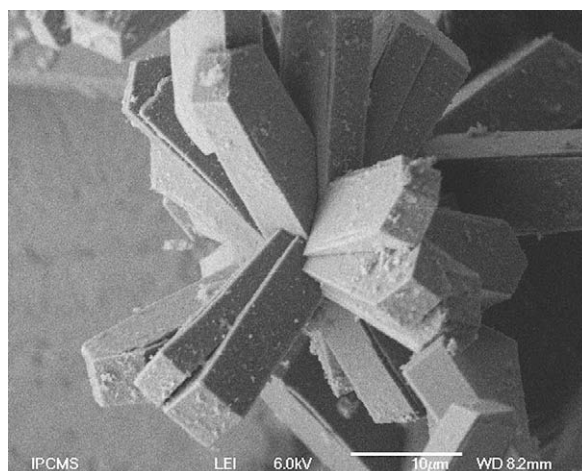


Fig. 3. Star-like morphology of F-MFI zeolite with aerosil 130 source.

Large prismatic crystals are usually reported for ZSM-5 zeolite, when TEOS was used as a silica source in the gel precursor [20]. Figs. 3 and 4 show SEM images of as-synthesized materials with polymeric aerosils 130, 200 and 300 sources. The zeolite crystals assemble to form a star-like morphology, which has never been reported so far for zeolite prepared in fluoride medium. These intergrown crystals with a nodal point are resistant to sonication during 30 min, which indicates a strong binding among the crystals. Complete transformation of the polymeric silica into zeolite was reached aside of the difference between their respective SSA. Indeed, the polymeric aerosil 130, having the lower SSA, reached complete nucleation of zeolite crystallites upon its surface.

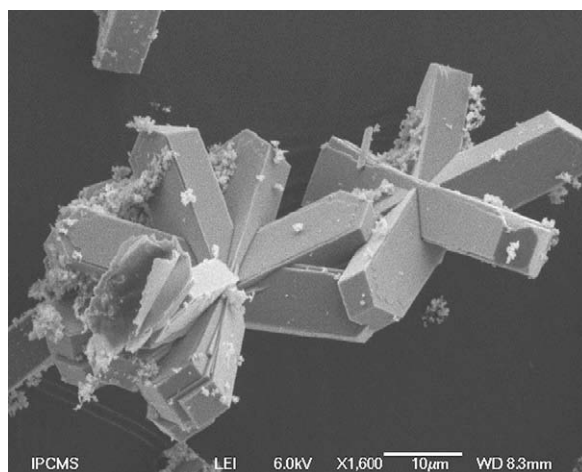


Fig. 4. Star-like growth of F-MFI material with aerosil 300 source.

In spite the differences between the SSA of three polymeric silica, aerosil used in this work, their formed zeolite crystals exhibit the same morphology (SEM micrographs), in a star-like manner. Nonetheless, we note that the polymeric silica with the high SSA: $300\text{ m}^2/\text{g}$ (aerosil 300), formed zeolite crystals in a reduced time compared to the two other aerosil silica (aerosils 200 and 130).

Fig. 5 shows the SEM micrograph of zeolite auto-assembled nanocrystals grown on SiC via fluoride-mediated synthesis. Nanofibers of ZSM-5 zeolite with a size of 90 nm and lengths up to several microns were obtained via *in situ* silicon carbide support self-transformation. The mechanical anchorage of as-synthesized zeolites on the SiC surface was checked by submitting the composite to a sonication treatment for 30 min. No subsequent zeolite loss could be observed after such treatment. The strong anchorage of as-grown zeolite crystals can be explained by the existence of a strong interaction between the formed SiOx layer on SiC (after activation) and the protonated H-ZSM-5 zeolite.

Consequently, the morphology of the crystal assembly is highly sensitive to the silica source, as already observed by Shantz and Lee in the synthesis of zeolites via cationic microemulsion [24].

3.2. Tentative mechanism for the ZSM-5 growth in a star-like manner

Coated ZSM-5 crystals on the SiC surface are the result of an individual crystal growth. However, these crystals obtained from barely soluble polymeric silica (aerosils 300, 200 and 130) are intergrown, and focused our interest in this work. Beside, seed effect in

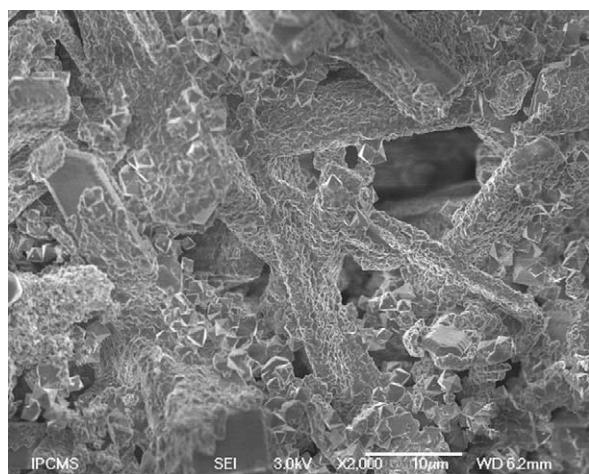


Fig. 5. SEM micrograph of zeolite auto-assembled nanocrystals grown on SiC via fluoride-mediated synthesis (147 h).

zeolite crystal growth is usually attributed to the presence of pure crystalline phase in the zeolite gel precursor [39]. The template effect is generally induced by totally solubilized species in the synthesis gel [39]. Since the silica sources used in this work, activated SiC substrate and polymeric silica gel, are not crystalline and barely soluble, one can exclude their templating or seeding effect.

The generally accepted model developed by Barrer et al. [25] supposing the formation of zeolite crystals in solution; i.e. the nucleation and growth of crystalline nuclei as a result of condensation reactions between soluble species; acts as a starting point for our study. The gel plays only a limited role, acting as a reservoir of matter. However, in our “*in situ*” procedure, where the silica source is provided by the support surface containing silica species (polymeric aerosil or β -SiC surfaces), one can presume a reorganization of the gel via solid–solid transformations [26]. The formation of self-structured zeolite in the present study seems to involve an aggregation mechanism based on a layer-by-layer Gibbs–Volmer growth model where a growth unit is adsorbed on a preferential crystal face, and migrates to find its optimum location [27].

However, it is generally admitted that there is a geometrical tuning between the template cations and the silica channel system. Burkett and Davis have evidenced the existence of van der Waals interactions between quaternary ammonium cations and the inorganic silica species [28], thus inducing the assembly of these organomineral moieties and the growth of this nuclei. A template cation is envisaged as being attached at the surface site of amorphous silica particle. Monomer units from the solution then join the growth site and assemble in an ordered array. The aggregate may behave as a nutrient–recipient pair in consistency with Thompson’s “tugging-chain” mechanism [29].

Nevertheless, the T–O–T bond making and bond breaking (where T = Si or Al), based upon nucleophilic reactions, facilitate structural modification catalysed by fluoride ions. The use of fluorides as mineraliser instead of the conventionally used hydroxide ion has presented a significant breakthrough in the field of zeolite synthesis [30–32]. The mineralising strength of F^- is less than that of OH^- , thus the solubilities and effective supersaturation are lower. Furthermore, it appears that this innovative strategy of using the self-transformation of barely soluble polymeric silica and β -SiC support, allows the formation of zeolite crystals, which can grow in peculiar directions and hence produce defined microstructures. We have successfully demonstrated that zeolite nanocrystals can, by themselves, build

a star-like network. Finally, our approach can open new routes toward the synthesis of novel zeolite structures and hence a combination of their nano/micro-organization on a macro-shaped support surface.

3.3. Catalytic activity

Light olefins, like ethene, propene, and butenes, are important building blocks for the chemical industry. Such olefins are mostly produced by steam cracking of naphtha and light alkane feedstocks at high temperatures even up to 1073 K. These processes are highly energy demanding and less effective due to their thermal cracking character. Catalytic cracking of naphtha and catalytic transformation of methanol (which could be obtained from natural gas) have attracted attention for the development of alternative processes for light olefin production.

The catalytic activity of the obtained materials (ZSM-5/SiC composite) was investigated in the conversion of methanol into hydrocarbons [33–35]. The steady-state conversion of methanol was reached after 2 h and was about 38%. For comparison, under the same experimental conditions, Zaidi and Pant have found the same level of methanol conversion with an

industrial H-ZSM-5 zeolite [36]. The selectivity toward the reaction products is shown on Fig. 6. During the first 2 h of the reaction, the ZSM-5/SiC composite exhibited a high selectivity (between 85 and 90%) toward saturated hydrocarbons with more than five carbon atoms chain length (C_{5+}). This composite made of zeolite nanofibres appears to be an active and selective (at least during 2 h) catalyst for the MTG reaction. However, after the initial period, the selectivity changed toward light saturated hydrocarbons C_1 – C_4 fraction (90% after 6 h of reaction). Surprisingly, no products in the range C_5 – C_{10} can be detected after 6 h, but only C_{10} , C_{11} and C_{12} were present. This phenomenon, so-called “window effect” has been observed for zeolites with smaller cages [37]. This intrinsic phenomenon to zeolite was reported for the first time by Goring [37]. Goring imputes such original behavior to the diffusion of linear hydrocarbons through the zeolite channels, depending on their carbon number (chain length). Nevertheless, recently Ruthven [38] suggested that the effect of heat transfer and isotherm non-linearity have to be privileged. The change in selectivity during the course of reaction has not been fully understood yet. However, it is possible to anticipate the changes in the zeolite channel

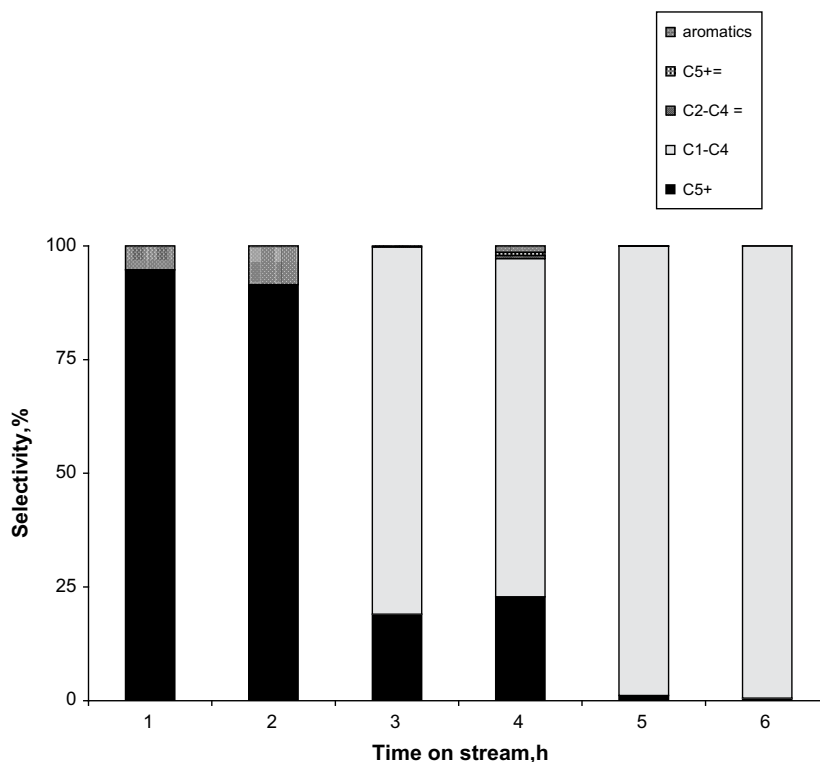


Fig. 6. Selectivity toward the different products (H-ZSM-5/SiC) at 673 K.

accessibility, similarly to that observed during the methane dehydroaromatization reaction over the ZSM-5 catalyst. In the present work, the change in selectivity toward the products is probably connected to micropore plugging via acidic condensation by hydrocarbon deposits, which can undergo isomerization-cracking reactions (mainly C₁–C₄ formed).

A preliminary test on the catalytic reactivity of the obtained H-ZSM-5 star-like (200 mg) was investigated in the liquid phase acylation of toluene (69 mmol) with benzoyl chloride (25 mmol) at 383 K under reflux conditions. The intergrown star-like ZSM-5 crystals exhibit a 98% selectivity toward the *para*-isomer, likewise isolated ZSM-5 crystals. Nevertheless, the zeolite crystals with the star-like morphology exhibit a higher activity than isolated MFI crystals (the difference is about 25% in favour of the assembled MFI crystals). Further studies are in progress to confirm this peculiar behavior in catalysis.

4. Conclusion

Self-structured MFI zeolite crystals were prepared under acidic conditions via *in situ* barely soluble polymeric silica or silicon carbide support self-transformation. ZSM-5 zeolites with high degrees of crystallinity were grown on the surface of β-SiC by consuming part of pristine support. A complete self-transformation was reached for the polymeric aerosil silica into organized zeolite assemblies in a star-like manner.

The novelty of our approach consists in the preparation of these zeolite structures without any external agent use. Finally these materials were catalytically active in the conversion of methanol-to-gasoline range hydrocarbons (MTG process), and thus exhibit the typical solid acidity of MFI zeolite.

Acknowledgments

The authors thank T. Romero, C. Marichal and S. Rigolet for their technical assistance. The authors are grateful to Degussa Evonik, more precisely Aerosil & Silanes Business unit for kindly providing silica and alumina sources.

References

[1] A. Cybulski, J.A. Moulijn (Eds.), *Structured Catalysts and Reactors*, Marcel Dekker, New York, NY, 1998.
 [2] B. Louis, P. Reuse, L. Kiwi-Minsker, A. Renken, *Appl. Catal. A* 210 (2001) 103.
 [3] H.P.A. Calis, A.W. Gerritsen, C.M. van den Bleek, C.H. Legein, J.C. Jansen, H. van Bekkum, *Can. J. Chem. Eng.* 73 (1995) 120.

[4] G.B.F. Seiger, O.L. Oudshoorn, A. Boekhorst, H. van Bekkum, C.M. van den Bleek, H.P.A. Calis, *Chem. Eng. Sci.* 56 (2001) 849.
 [5] S. Mintova, V. Valtchev, L. Konstantinov, *Zeolites* 17 (1996) 462.
 [6] J. Sterte, J. Hedlung, D. Creaser, O. Ohrman, W. Zheng, M. Lassinantti, Q. Li, F. Jareman, *Catal. Today* 69 (2001) 323.
 [7] B. Louis, C. Tezel, L. Kiwi-Minsker, A. Renken, *Catal. Today* 69 (2001) 365.
 [8] R. Lai, Y. Yan, G.R. Gavalas, *Microporous Mesoporous Mater.* 37 (2000) 9.
 [9] V. Valtchev, S. Mintova, B. Schoeman, L. Spasov, L. Konstantinov, *Zeolites* 15 (1995) 527.
 [10] M.A. Ulla, R. Mallada, J. Coronas, L. Gutierrez, E. Miro, J. Santamaria, *Appl. Catal. A* 253 (2003) 257.
 [11] M.A. Ulla, E. Miro, R. Mallada, J. Coronas, J. Santamaria, *Chem. Commun.* (2004) 528.
 [12] M.J. Ledoux, J. Guille, S. Hantzer, D. Dubots, US 4914070, Pechiney; 1990.
 [13] M.J. Ledoux, C. Pham-Huu, *Cattech* 5 (2001) 226.
 [14] F.C. Patcas, *J. Catal.* 231 (2005) 194.
 [15] M.J. Ledoux, C. Pham-Huu, *Catal. Today* 15 (1992) 263.
 [16] B. Louis, S. Walspurger, J. Sommer, *Catal. Lett.* 93 (2004) 81.
 [17] D.S. Wragg, R. Morris, A.W. Burton, S.I. Zones, K. Ong, G. Lee, *Chem. Mater.* 19 (2007) 3924–3932.
 [18] S.I. Zones, A.W. Burton, G.S. Lee, M.M. Olmstead, *J. Am. Chem. Soc.* 129 (2007) 9066–9079.
 [19] J.L. Guth, L. Delmotte, M. Soulard, N. Brunard, J.F. Joly, D. Espinat, *Zeolites* 12 (1992) 929.
 [20] C. Baerlocher, W.M. Meier, D.H. Olson, *Atlas of Zeolite Framework Types*, fifth ed., Elsevier, Amsterdam, 2001.
 [21] G. Engelhardt, D. Michel (Eds.), *High-Resolution Solid State NMR of Silicates and Zeolites*, John Wiley and Sons, Chichester, 1997.
 [22] K.J.D. Mac Kenzie, M.E. Smith, *Multinuclear Solid-State NMR of Inorganic Materials*, In: *Pergamon Materials Series*, vol. 6, Pergamon, Oxford, 2002.
 [23] J.P. Tessonnier, B. Louis, S. Walspurger, J. Sommer, M.J. Ledoux, C. Pham-Huu, *J. Phys. Chem. B* 110 (2006) 10390.
 [24] S. Lee, D.F. Shantz, *Microporous Mesoporous Mater.* 86 (2005) 268.
 [25] R.M. Barrer, J.W. Buynham, F.W. Bultitude, W.M. Meier, *J. Chem. Soc.* (1959) 195.
 [26] E.G. Derouane, S. Detremmerie, Z. Gabelica, N. Blom, *Appl. Catal.* 1 (1981) 201.
 [27] S. Ivanova, B. Louis, M.J. Ledoux, C. Pham-Huu, *J. Am. Chem. Soc.* 129 (2007) 3383.
 [28] S.L. Burkett, M.E.J. Davis, *Phys. Chem.* 98 (1994) 4647.
 [29] R.W. Thompson, in: H.G. Karge, J. Weitkamp (Eds.), *Molecular Sieves*, Springer-Verlag, Berlin, 1998.
 [30] E.M. Flanigen, R.L. Patton, US 4073865; 1978.
 [31] J.L. Guth, H. Kessler, J.M. Higel, J.M. Lamblin, J. Patarin, A. Seive, J.M. Chezeau, R. Wey, *Zeolite Synthesis*, ACS Symposium Series, Washington DC, 1989, 176.
 [32] B. Louis, L. Kiwi-Minsker, *Microporous Mesoporous Mater.* 74 (2004) 171.
 [33] C.D. Chang, *Catal. Rev. Sci. Eng.* 25 (1983) 1.
 [34] M. Stöcker, *Microporous Mesoporous Mater.* 29 (1999) 3.
 [35] G.F. Froment, W.J.H. Dehertog, A.J. Marchi, *Catalysis* 9 (1992) 1.
 [36] H.A. Zaidi, K.K. Pant, *Catal. Today* 96 (2004) 155.
 [37] R.L. Goring, *J. Catal.* 31 (1973) 13.
 [38] D.M. Ruthven, *Microporous Mesoporous Mater.* 96 (2006) 262.
 [39] L. Tosheva, V. Valtchev, *Chem. Mater.* 17 (2005) 2494.